ORIGINAL ARTICLE

Suitability of excavated London clay as a supplementary cementitious material: mineralogy and reactivity

Yuvaraj Dhandapani · Alastair T. M. Marsh · Suraj Rahmon · Fragkoulis Kanavaris · Athina Papakosta · Susan A. Bernal

Abstract This study evaluated the potential of producing supplementary cementitious materials (SCMs) using London Clay excavated from construction activities of the High Speed 2 rail project. A trade-off between enhancing reactivity versus decomposition of impurities (e.g., pyrite, carbonates) present in different London Clay samples was considered in selecting the calcination temperature. The additional reactivity obtained by calcining at 800 °C is deemed to be worth the cost of the small additional process emissions from decomposition of carbonate minerals. Blended cement formulations were developed with the produced SCMs, with replacement levels of 50 and 70 wt%. The optimal gypsum dosage was found to be 1 wt%, which resulted in improved reaction kinetics at early ages. Mortars produced with these binders developed ~ 50 MPa compressive strength after 90 days of curing even with 70 wt% replacement, which is sufficient for potential production of low to medium strength concretes. These findings demonstrate the excellent potential of London Clays for SCM production and present a systematic approach for characterisation, processing and utilization of excavated mixed clays obtained from infrastructure projects.

Keywords Excavated material · Calcined clays · Supplementary cementitious materials · Reactivity

Y. Dhandapani · A. T. M. Marsh · S. Rahmon · S. A. Bernal (✉)
School of Civil Engineering, University of Leeds, Leeds LS2 9JT, UK
e-mail: s.a.bernallopez@leeds.ac.uk

F. Kanavaris (✉)
Technical Specialist Services, Materials, ARUP, London, UK
e-mail: Frag.Kanavaris@arup.com

A. Papakosta
Skanska Costain Strabag (SCS) Railways JV, London, UK

1 Introduction

The construction industry faces many challenges to reduce its environmental impacts, including reducing the volume of construction waste, and particularly the volume of waste sent to landfill. In Europe, excavated soils are the largest stream of construction waste, estimated to be < 500 MT/year [1]. In the UK, there is a target to reduce excavation soil sent to landfill by 75% by 2040, and zero soil to landfill by 2050 [2]. Whilst some of this material can be reused for geotechnical activities elsewhere on site, transportation of excavated soil to landfill is still a common practice [3]. Volumes of excavated material are particularly large for major infrastructure projects

involving tunnelling—hundreds of megatonnes of excavated material are forecast to be generated over the next 50 years [4]. Where excavation is carried out in urban areas, transport of excavated soil out of the site can add disruption to local residents. The overall management of excavated soil can be improved by increasing their use in construction materials [5].

Another challenge is to reduce the embodied carbon of construction, with particular scrutiny on concrete. In the UK, the Low Carbon Concrete Group roadmap targets net zero emissions from concrete production by 2050, with at least a 50% reduction to be achieved by 2030 [6]. One of the fastest ways to decrease the carbon footprint of cement is to decrease the clinker content with higher substitutions of supplementary cementitious materials (SCMs) [7]. Blast furnace slag and fly ash remain the most commonly used SCMs in the UK. However, falling domestic supply and an increased reliance on imports are expected to reduce supply chain resilience and increase prices in the coming years [8]. The use of calcined clay in binary and ternary forms (with limestone) has the potential to reduce the CO_2 footprint of cementitious materials between 30 and 50% compared to Portland clinker [9–11]. Therefore, calcined clays produced from clays with low purity and/or mixed clay mineralogy are increasingly being explored as an alternative to conventional SCMs. However, their variation in purity and mineralogy raises questions around selection of calcination conditions to promote optimum reactivity, how the properties of such calcined clays might influence fresh, mechanical or long-term performance of concretes produced with them, compared with materials produced with other SCMs.

The use of excavated clayed soils as a SCM offers an opportunity for the construction industry to address the mentioned challenges simultaneously. Design of mobile calcining plants for clays or soils has been proposed [12, 13]. However, an integrated calcining, grinding and blending plant on-site has not yet been implemented on any major construction operations. An innovative mobile clay processing facility is currently under development as part of a major infrastructure project in the UK [14]. This set-up would have numerous benefits in principle, including reducing the volume of excavated material sent to landfill; improving the functional value of soils, relative to use in groundworks or landfill; reducing the flow of materials entering and leaving the construction site, and reducing the impact of truck traffic on the neighbourhood. There is increasing research interest in adopting resource recovery principles in the construction lifecycle in order to reduce environmental impacts [15]; however, excavated clays have received little attention so far.

Several routes for valorisation for excavation waste have been investigated, which include the developed of supplementary cementitious materials [16–18], as fine aggregates [5, 19], for development of earth-based materials [20, 21], as precursors of alkali-activated cements production [22] and as raw feeds for calcium sulfoaluminate (CSA) cements production or as CSA replacements [23, 24]. Wherever possible, excavation wastes should be used as raw material in earth construction due to the low embodied carbon of the process, however, experience has shown that excavation management is a common problem in major infrastructure projects, particularly in densely populated areas, e.g., an artificial island was created from waste from a past major infrastructure [25].

This study investigated the feasibility of producing SCMs using excavated material from ongoing tunnelling works in the Greater London region, whilst the excavated material predominately consists of London Clay formation. These works are linked to the first part of High Speed 2 (HS2, https://www.hs2.org.uk), a major rail infrastructure project in the UK [26] and it is estimated that over 5 million m^3 of material will be excavated—the majority of this is expected to be London Clay [16].

London Clay is the name given to the type of clays found in the London Basin geological formation. They are mixed, or common, clays—their clay mineral assemblage typically consists of smectite, illite, kaolinite and chlorite [27]. This diversity within the clay mineral fraction makes London Clays mineralogically distinct from kaolinitic clays, which have received most attention within the field of calcined clays as SCMs. Crucially, their kaolinite content is relatively low—broadly within the range of 10–30 wt% [27]. This is believed to be disadvantageous from an SCM production perspective, as 40 wt% of kaolinite content has previously been established as the optimal amount required [28, 29] to produce blended cements with equivalent strength development by 7 days to that of Portland cement systems. However, the extent to which the other, less reactive clay minerals typically present in London Clays (i.e.

smectite, illite, chlorite) may contribute to reactivity is still an open research question.

Non-kaolinitic clay minerals are also known to exhibit pozzolanic reactivity once calcined, however, they are typically less reactive than metakaolin [30–33]. Recent work on common clays from Germany determined that smectite and interstratified illite–smectite make a tangible contribution to overall reactivity [34]. The only peer-reviewed study so far specifically on the use of London Clays as SCMs found that calcination at 900 °C for 2 h gave the best reactivity performance at 14 days and beyond, as measured by the Frattini test, portlandite consumption measurements and strength activity index; however, these findings are related to clays calcined in 5 cm diameter pellets in laboratory scale. Concretes with 30 wt% replacement using London Clay calcined at 900 °C developed sufficient workability (i.e., Slump class 2, 50–90 mm slump) and a satisfactory performance in terms of 90-day compressive strength [18]. Another study on clays with < 20 wt% kaolinite content from a variety of UK geological formations (but not including the London Clay formation) deemed them to be promising as potential SCMs [35]. Whilst the small amount of literature on the use of London Clays as SCMs shows promise, more research is needed in order to gain a comprehensive understanding of the links between mineralogy, calcination conditions, and performance in cementitious systems.

Beyond the role of the clay minerals, the associated minerals typically found in London clays also present challenges including ensuring that sulphur-bearing phases (e.g. pyrite) in the as-received material do not pose a durability threat after calcination, and ensuring that carbonate minerals (e.g. calcite, dolomite) do not decompose to form problematic amounts of expansive phases (e.g. free lime, periclase). Free lime and MgO are also known to cause expansion due to crystallization of calcium hydroxide and magnesium hydroxide [36, 37]. Provided that calcination conditions are sufficient to cause complete thermal decomposition of iron sulphide phases, then their presence in an as-received clay is not problematic [38]. Aside from associated minerals, it is feasible that remnants of polymer foams used for facilitating excavation may be present in excavated material. It is important to assess the calcined excavated materials to ensure that no such

materials remain which might have a detrimental effect on use in concrete.

In this study three different sample locations of excavated London Clay were investigated. These materials were selected to indicate the extent of variability of the spoils being generated from HS2 excavation works in the Greater London area. Detailed characterisation of the clayed soils was conducted using a multi-technique approach including X-ray fluorescence spectroscopy (XRF), quantitative X-ray diffractometry (XRD) and thermogravimetry analysis coupled with mass spectrometry (TG-MS). Different calcination conditions were applied to these materials in order to enhance their chemical reactivity, which was determined by the R^3 testing method. Changes in the mineralogy and structure of the excavated materials upon thermal treatment were evaluated applying similar techniques to those used for characterising the raw clays.

Blended Portland paste mixes were optimised (gypsum adjustment) and produced with high replacement levels (50 and 70 wt%) using selected calcined clays. The kinetics of reaction of these mixes were determined using isothermal calorimetry. Compressive strength testing in mortars specimens was also conducted.

2 Materials and methods

2.1 Materials

Samples of excavated materials were sourced from three different HS2 construction sites, within the Greater London area (Fig. 1). All sites fell within an area with a radius of 6 km. The extraction depths were 11 m for the Westgate site, 23 m for the Euston site, and between 3 and 30 m depth for the Victoria site.

Chemical analysis of the raw clays was conducted using X-ray fluoresce (XRF) spectroscopy, carried out with a Rigaku ZSX Primus II, using a fused bead preparation method and a loss on ignition (LOI) step at 900 °C. The chemical oxide compositions (determined by XRF) of the raw clays were broadly similar (Table 1). Differences in Al_2O_3 and CaO indicated potential small differences in quantities of clay minerals and carbonates.

For the production of Portland blended mixes, a commercially available CEM I 42.5R Portland cement
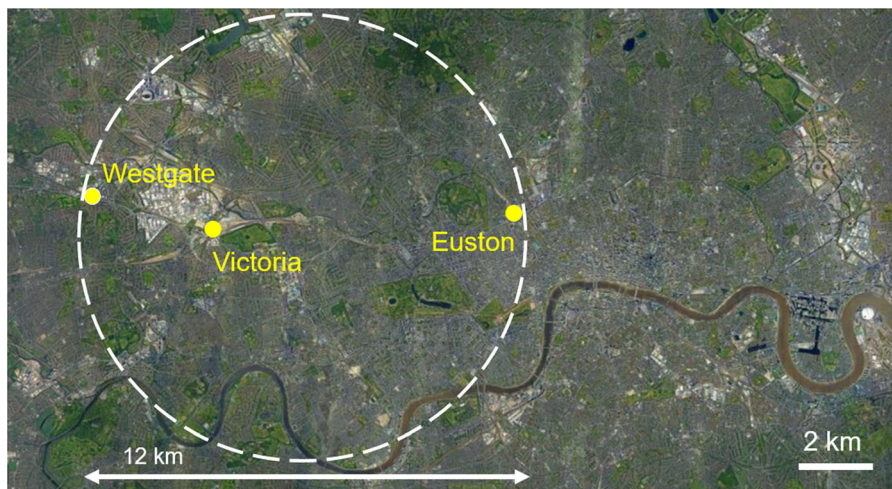
Fig. 1 Locations of HS2 construction sites within Greater London from where samples of excavated material were sourced

Table 1 Oxide compositions of the raw clays, determined by XRF

Clay ID	SiO_2	Al_2O_3	Fe_2O_3	K_2O	MgO	CaO	TiO_2	SO_3	Na_2O	P_2O_5	Other (< 0.1 wt%)	LOI*
Westgate	53.51	13.89	6.10	2.74	2.62	6.30	0.81	0.96	0.33	0.21	0.24	12.30
Euston	56.97	15.75	6.37	3.31	2.86	2.04	0.91	0.91	0.46	0.18	0.26	10.00
Victoria	53.42	17.07	7.02	3.37	3.38	2.05	1.00	0.94	0.49	0.17	0.28	10.80

*LOI stands for loss on ignition determined at 900 °C for 2 h

(from Cementos Alfa) and laboratory-grade gypsum (Calcium sulfate dihydrate, 99%, Alfa Aesar) were used. Visocrete 600 MK (from SIKA Ltd.) was used as a superplasticiser to increase fluidity of the mortars prepared with blends.

2.2 Methods

2.2.1 Processing and calcination

Before describing the detailed steps of processing and calcination, a brief clarification of terminology will be given. Hereon, "as-received clay" is used to refer to the extracted material, before initial drying; "raw clay" is used to refer to the clay after being air-dried, crushed and homogenised; "calcined clay" is used to refer to the clay after being calcined in a laboratory furnace and ground in a laboratory ball mil, and "industrially calcined clay" is used to refer to the clay after being calcined in a pilot scale rotary kiln and and an industrial ball mill.

The as-received clay was manually broken into small pieces, and then dried out in shallow trays in 40 °C oven for 24 h to reach an 'air dry state' in line with BS 1377-1:2016 [39]. This was necessary to allow the as-received material to be crushed and homogenised. Moisture content was measured according to BS 1377-2:1990 [40], with three samples of > 30 g of material taken from different locations in the as-received clay, and dried at 105 °C for 24 h. Moisture content calculated from mass loss was then expressed as a percentage of the dry clay mass.

Whilst most focus of the embodied carbon of calcined clays is on the heating required for the calcination step, the moisture content of clays has a substantial influence on the energy required for drying before calcination [41]. Moisture content is expressed as a percentage of the dry clay mass in the soil and the results varied between 20 and 45%, as summarised in Supplementary Information (Table S1). These values showed substantial variation in moisture content between the different clay sources. While it is not

viable to conduct a cradle-to-gate analysis of embodied carbon, given the hypothetical nature of the processing set-up, these findings demonstrate that whilst the overall mineralogy between the clays did not vary greatly, differences in ground conditions could result in different energy demands for drying excavated material from different sources. It is also worth noting that apart from the ground conditions, the moisture content of soils/clays could be influenced by their storage conditions after excavation (i.e. exposure to rainfall), or even by drilling agents (e.g. polymer foams used to facilitate excavations).

The 'air dry' material was then passed through a jaw crusher (Retsch BB200) until all material passed through a 10 mm sieve. This 10 mm upper size limit was based on recommended feed size for a rotary kiln, to align the laboratory process with the industrial process as far as feasible. A riffle box was then used to homogenise and obtain representative samples of material from the whole. For generating finely powdered material for characterisation, a small sample of $\sim$ 1 wt% of the whole was taken, and wet-ground in isopropanol until < 125 μm.

Clays were calcined in a laboratory static furnace (Carbolite AAF 1100), using a dwell time at peak temperature for about 1 h, and a temperature of either 700 or 800 °C. These temperatures were selected based on the range of dehydroxylation temperatures identified via thermogravimetric analysis [42] (Sect. 3.1). Clays were loaded in shallow porcelain crucibles. After calcination, the clay was then ground for 1 h in a laboratory roller ball mill, using ceramic grinding balls. This was undertaken to achieve a desirable particle size distribution for supplementary cementitious materials (d_{50} < 20 μm and d_{90} < 100 μm) that is typical for use in cementitious materials [30].

For the development of blend formulations, about 300 kg of London Clay from the Westgate site was industrially calcined (IC) in a rotary kiln (hereafter referred to as Westgate-IC). The Westgate clay was selected on the basis of logistical convenience of sourcing larger quantities of material within the planned works schedule. The as-received Westgate clay was granulated into smaller pieces, calcined in a rotary kiln at 800 °C with a residence time of 1 h, and subsequently ground in a ball mill. Figure 2 shows the size and colour of the clay at different stages of pre-

and post-calcination. Characterisation data for Westgate-IC is included in the Supplementary Information.

2.2.2 Characterisation

After processing of the clays, the following analyses were performed:

XRD patterns were collected using a Panalytical Empyrean diffractometer (45 kV, 40 mA), using a range of 4–70°2θ, and a step size of 0.0131°2θ. X'pert Highscore plus V5.1 was used for phase identification using PDF-4 + 2022 ICDD database. Identification of mineral phases was aided by reference to Kemp and Wagner [27], and mineral abbreviations were used in line with Clay Minerals Society nomenclature described in Warr [43]. The diffractograms obtained from XRD were used to investigate the mineral phase assemblages via Rietveld refinement, using the external standard method where pure corundum (> 99% purity Al_2O_3) was tested separately at the same conditions, and used as an external standard for analysis using the K-factor obtained from the standard for estimation of amorphous content. Structure files from the 2022 ICDD PDF-4 + database were used for fitting. Due to lack of Powder Diffraction File (PDF) structure files for the clay mineral montmorillonite, its low angle (< 10°2θ) 001 reflection was excluded from the analysis—it was hence treated as part of the background intensity. Due to limitations on the availability of structure files for 2:1 clays, the structural file for a muscovite (a micaceous mineral) was used to fit the illite peaks. Hence, the results for the proportions of minerals present in the bulk are semi-quantitative.

TG-MS measurements were conducted using a Netzsch STA 449 F5 coupled with a Netzsch QMS 403D mass spectrometry unit. 20 ± 1 mg of sample was used for each measurement, using an alumina crucible. Samples were evaluated between 30 and 1000 °C using a heating rate of 10°C/minute, under nitrogen atmosphere using a flow gas rate of 60 mL/min. Kaolinite and carbonate contents of the source clays were estimated using the method described by Snellings et al. [42]. For kaolinite, a threshold range of 400–600 °C was used for calculating dehydroxylation mass loss; for carbonates, a threshold range of 600–800 °C was used for calculating the mass loss due to thermal decomposition. Mineral content estimates were calculated as wt% values, with respect to

Fig. 2 Photographs of the Westgate clay at various stages of the industrial calcination process, with approximate scale bars to indicate changes in feed and particle size

the dry mass of each clay (defined here as the mass at 250 °C). Estimates of uncertainty were made by varying the threshold temperatures ranges to plausible minimum (400–550 °C for kaolinite, and 625–775 °C for carbonates, respectively) and maximum (300–625°C for kaolinite, and 600–825 °C for carbonates, respectively) ranges.

Particle size distribution (PSD) measurements were conducted using a Malvern Mastersizer 3000, using a dispersing unit at a rotation speed of 1400 rpm. An in-situ ultrasonication treatment of 5 min was carried out before each measurement. Average values were calculated for each sample from 10 measurements of 4 s duration. For clays, a dispersal medium of dionised water was used, using a pinch of sodium hexametaphosphate as a dispersal agent. The optical parameters used were refractive index = 1.56, and absorption coefficient = 0.01 [44]. For the cement powder, isopropanol was used as the dispersing medium, and measurement were collected using a refractive index = 1.7, and absorption coefficient = 0.1 [44].

To determine the chemical reactivity of the calcined clays, the evolved heat method referred to as R^3 test was adopted according to the ASTM C1897-20 [45] standard, using a TAM Air calorimeter. The reactivity thresholds established specifically for calcined clays based on 7-day cumulative heat values [46] were used to classify the calcined clays assessed in this study according to their chemical reactivity category.

To develop an understanding of how clay mineralogy affects calcined clays' chemical reactivity determined according to the R^3 testing method, a series of reference clays were also tested. C–K is a kaolinitic clay, calcined at 800 °C. Suplementary information reporting chemical composition and thermogravimetric analysis of the

C–K is made available in Table S6 and Figure S1, respectively. This was selected to be a point of comparison, as it is a kaolinitic clay with similar kaolinite content ($\sim$ 27 wt%) to the three London Clays used in this study, but only quartz as remaining fraction, enabling to identify the contribution of kaolinite reactivity alone. In addition, a series of manufactured metakaolins were made, by blending an industrially sourced, high-purity metakaolin (Imerys Metastar 501) with quartz. These were selected to provide a hypothetical trend line, for how kaolinite content might be expected to influence the chemical reactivity of calcined clays. Characterisation data for these clays is provided in the Supplementary Information.

2.2.3 Blended cement formulations and compressive strength assessment

Two replacement levels of industrially calcined Westgate clay (Westgate-IC) were chosen to work with for mix design development: 50 wt% and 70 wt%. These will subsequently be abbreviated as "CC50" and "CC70". The main reasons why this research is limited to study binary mixes with calcined clay are: (i) Enable the higher waste clay re-utilisation possible and consequently minise the volumes of spoil ending in landfill, (ii) Compliance with UK standards which permits calcined pozzolana to replace up to 55% of CEM I while ternary mixes with limestone are not included, and (iii) Less complication on-site as using a ternary binder adds greater complexity for on-site production with sourcing, grinding and blending of limestone.

For each replacement level, the influence of gypsum addition (0, 1, 3, 5 wt%) on reaction kinetics was investigated using isothermal calorimetry. For

determining the optimal gypsum addition for each calcined clay replacement level, isothermal calorimetry at 20 °C was carried out in a TAM Air calorimeter to study the hydration kinetics. Approximately 9 g of cement paste (6 g of binder + 3 g of water) was used for the calorimetry measurements, mixed in-situ using a vortex mixer for 2 min before placement inside the instrument. Gypsum addition was attempted as high volume replacement is known to create additional sulphate demand. The level of gypsum addition will be abbreviated as using a "-GN" suffix, where N refers to the % of gypsum addition. Details of the blend composition is summaried in Table 2

To assess the effect of different replacement levels of calcined clay on setting time, a Vicamatic 2 (CONTROLS S.p.A.) automated Vicat tester was used to measure setting time. Optimal blended formulations were then used to produce mortar specimens to determine the mechanical strength development of these materials after 2, 7, 28 and 90 days' curing. Compressive strength measurements were carried out on mortar cubes (50 × 50 mm), in line with BS EN 12390-3:2019 [47]. Mortar were prepared with CEN standardised sand with a cement: sand ratio of 1:3 and a water to binder ratio (w/b) of 0.5. Superplasticizer was added to ensure sufficient workability in the mortar based on the results reported elsewhere [48]. A MATEST compression instrument was used with a loading rate at 3000 N/sec, and average compressive strength values were calculated from three mortar cube specimens.

3 Results and discussion

3.1 Mineralogy of excavated clays

XRD patterns (Fig. 3) revealed broad similarities in the mineralogy of the three raw clays. All clays contained kaolinite, as well as the 2:1 clay minerals montmorillonite and illite. Dolomite and smaller amounts of calcite were present in all three raw clays. Minor/trace amounts of pyrite were present in all three of the raw clays, and minor/trace amounts of gypsum were present in the Westgate and Euston clays. Powder diffraction details of phase used for analysis are kaolinite (powder diffraction file (PDF), #01-075-0938 and 04-013-2815), muscovite (PDF# 00-058-2035), quartz (PDF# 00-046-1045), microcline(PDF#01-076-1238), calcite (PDF# 00-005-0586), dolomite (PDF# 00-036-0426), Gypsum (PDF# 00-021-0816), albite (PDF# 04-007-5466), pyrite (PDF# 01-071-3840), rutile (PDF# 00-021-1276).

These clay minerals were also identified by Zhou et al. [18] studying a London Clay and in other studies on common clays [34, 35]. A wide range of associated minerals can be found in clays, depending on their formation conditions [49]—the majority of associated minerals identified here have previously been observed in a range of different occurrences of London Clay [27]. Whilst kaolinite containing quartz occurs very frequently in clays used in the SCM literature, the other clays minerals present are not so well-understood.

The TG (Fig. 4) and dTG curves (Fig. 5a) of the raw clays were consistent with the mineral phases identified via XRD. Evolution of H_2O (Fig. 5a) over

Table 2 Composition of the blends used for identification of gypsum adjustment

Blend ID	CEM I 42.5R (wt%)	Calcined London Clay (Westgate-IC) (wt%)	Gypsum (wt%)
CC50–G0	50	50	0
CC50–G1	50	49	1
CC50–G3	50	48	3
CC50–G5	50	45	5
CC70–G0	30	70	0
CC70–G1	30	69	1
CC70–G3	30	67	3
CC70–G5	30	65	5

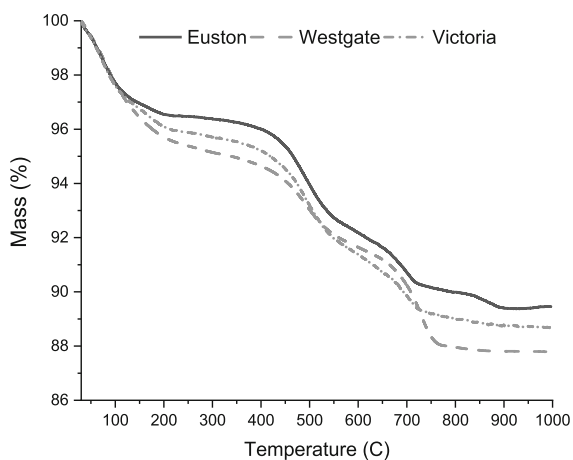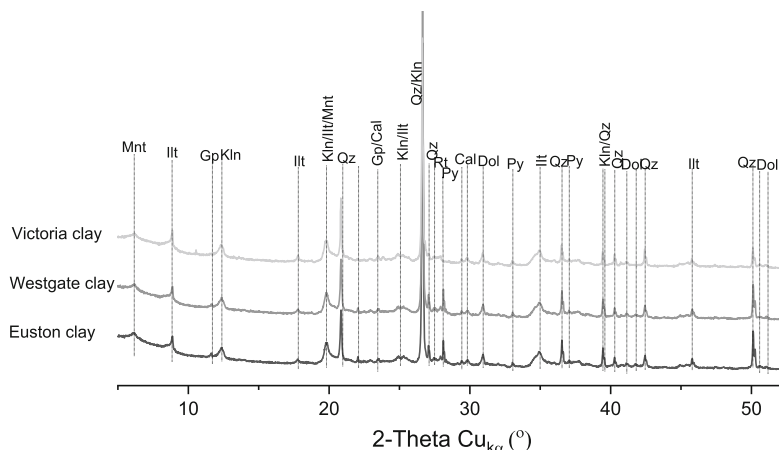Fig. 3 Cu-α XRD patterns for the raw clays. Abbreviations for clay minerals: *Mnt* montmorillonite, *Ilt* illite, *Kln* kaolinite. Abbreviations for associated minerals: *Qtz* quartz, *Cal* calcite, *Dol* dolomite, *Gp* gypsum, *Py* pyrite, *Rt* rutile
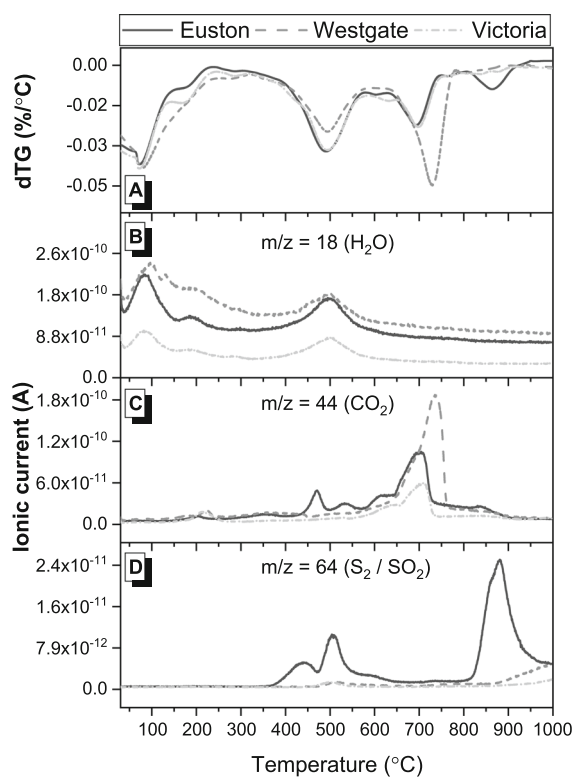

Fig. 4 Thermogravimetric curves for the raw London Clays

the range of 400–600 °C confirmed the presence of kaolinite in all three raw clays [50]. Evolution of CO_2 (Fig. 5b) over the range of 600–800 °C confirmed the presence of carbonate minerals (dolomite and/or calcite) in all three raw clays [50]. The more intense weight loss in this region for the Westgate clay indicated a higher content of carbonates. Evolution of S_2/SO_2 (Fig. 5c) over the range of 450–650 °C confirmed the presence of minor amounts of pyrite in all three raw clays [50], as previously identified by XRD (Fig. 3). Total mass loss at 1000 °C was in the range of 10.5–12.3%—this range indicates small differences in the quantities of each mineral present between the different clays.

Mineral phases of particular interest were kaolinite and carbonates (including both dolomite and calcite). From TG results (Fig. 4), an estimate was made using

Fig. 5 (a) Differential thermogravimetric curves, and mass spectroscopy curves of (b) H_2O evolution, (c) CO_2 evolution, and (d) S_2/SO_2 evolution for the raw London Clays

mass loss from TG for the quantities present in each of the three raw clays (Table S2 in the Supplementary Information). Whilst the Euston and Victoria clays present similar contents of kaolinite (about 28%), the Westgate clay had a slightly lower kaolinite content (i.e., 22%) and slightly higher carbonates content.

The optimal calcination temperature was anticipated to be a trade-off between an increased dehydroxylation of the kaolinite as well as amorphization of the 2:1 clay minerals (beneficial to reactivity), and decomposition of carbonate phases (deleterious to hydration) [18, 51]. Calcination temperatures of 700°C and 800°C were therefore selected, for a duration of one hour in a static laboratory furnace.

Clays with a mixed clay mineralogy and a range of associated minerals offer distinct characterisation challenges compared to kaolinitic clays. Firstly, there is likely to be some degree of overestimation in kaolinite content when using TG analysis. This is because non-negligible mass loss arises from other clay minerals and associated minerals, which occurs in the same temperature range as kaolinite dehydroxylation. This can be seen in the CO_2 and SO_2 evolved gas data which confirms the decomposition of carbonate and sulphate minerals in the 400–600 °C temperature range. TG-MS data presented (Fig. 5) shows the need to critically cross-link characterisation data when adopting the mass loss method [52] to estimate kaolinite content in complex clays. The same applies vice versa: it is likely that TG estimates for the content of carbonate minerals is an overestimate, given that its decomposition range overlaps with that of kaolinite.

### 3.2 Physical characteristics of calcined clays

On the basis of previous experience in the optimal particle size distribution of calcined clays [30], upper bounds of $d_{50} < 20$ μm, $d_{90} < 100$ μm were used as acceptable limits. All the calcined clays met these particle size requirements. $d_{50} < 20$ μm widely accepted range for cementitious materials that are used to substitute to Portland cement. The d_{50} and d_{90} values of the calcined clays after grinding are presented in Table S3, and particle size distribution curves are provided in Figure S2 in the Supplementary Information file, respectively.

3.3 Mineralogy of calcined clays

The crystalline minerals identified in all three clays after calcination at 700 and 800 °C were broadly similar, albeit with some differences (Fig. 6). Dehydroxylation of kaolinite was complete for all calcined clays, as seen from the absence of the kaolinite 001 peak at 12.4°2θ. A small amount of calcite was still detected after calcination at 700°C in all three clays, from the doublet peaks at 29.3 and 48.4°2θ. Negligible calcite was detected in the Euston and Victoria clays after calcination 800 °C, suggesting thermal decomposition was near-complete. However, a low intensity calcite peak was still detected in Westgate 800 °C, indicating that a small amount of calcite still remained after calcination at 800 °C, probably calcite formed from decomposition of dolomite to MgO and $CaCO_3$. Differing extents of carbonate decomposition with different calcination temperatures was also observed in a previous study [51].

No pyrite was detected in the calcined clays for all three clay sources, from the absence of characteristic peaks at 28.7 and 37.3°2θ. Instead, peaks associated with hematite (PDF# 04-015-9576) were observed at 33.1 and 35.6°2θ. This demonstrates the decomposition of pyrite to form hematite was completed at both calcination temperatures studied. This observation agrees with previous work which also showed that calcination above 650°C was sufficient to decompose pyrite [38]. This is an important finding which is particularly encouraging towards the adoption of calcined London Clay as an SCM in concrete, since pyritic clays are often deleterious for concrete elements [53]. Oxidation of pyrite (Fe_2S) has been known to release sulfate which could cause potential sulfate attack and also create acidic environment in the long-term exposure [54, 55]. Such sulfate attack due to pyrites present in sub-soil has been problematic in several regions of UK, US, and Canada [55, 56]. In the only previous study on calcination of London Clays [18], no calcite, dolomite or pyrite were identified in the raw clay, so there is no direct comparison to be made in this regard. This difference between the clays in these two studies is not surprising, as the presence of minor associated minerals is known to vary within the London Clay formation [27]. It is worth also noting that there might be occasions where clays are contaminated with other deleterious substances with regards to the durability of reinforced concrete, such as chlorides. Chlorides are expected to be found in clays in the vicinity of marine environments or in clays associated with saline groundwater conditions. In the particular case of London Clay considered herein, the samples investigated did not exhibit any significant chloride content, owing to the locations considered. In locations where London Clay is closer to the river
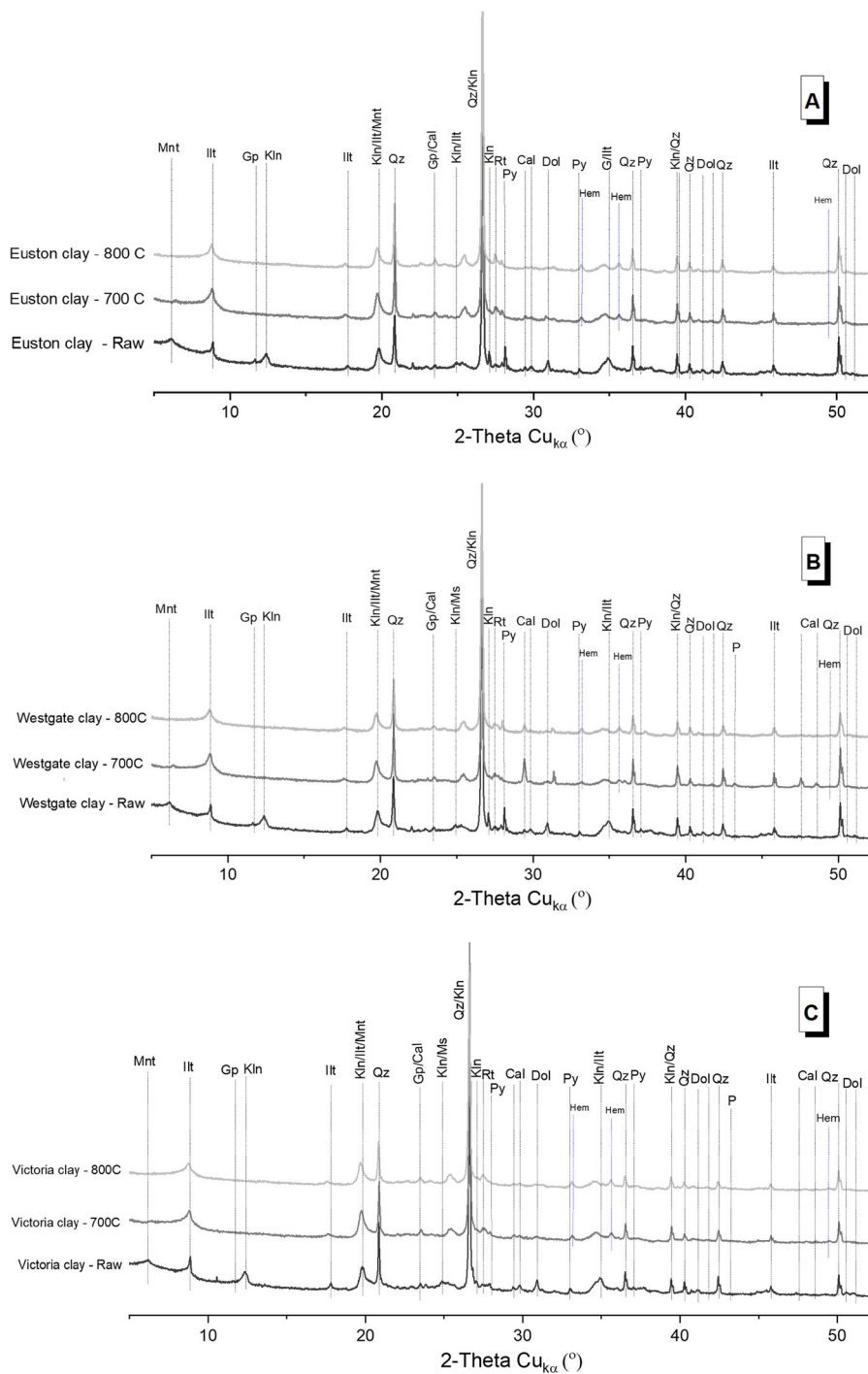
Fig. 6 Cu-α XRD patterns, before and after calcination, for (**a**) Westgate clay, (**b**) Euston clay, (**c**) Victoria clay. Abbreviations for clay minerals: *Mnt* Montmorillonite; *Ilt* Illite; *Kln* Kaolinite. Abbreviations for associated minerals: *Qtz* Quartz; *Cal* Calcite; *Dol* Dolomite; *Gp* Gypsum; *Py* Pyrite; *Rt* Ructile; *Hem* Hematite; *P* Periclase
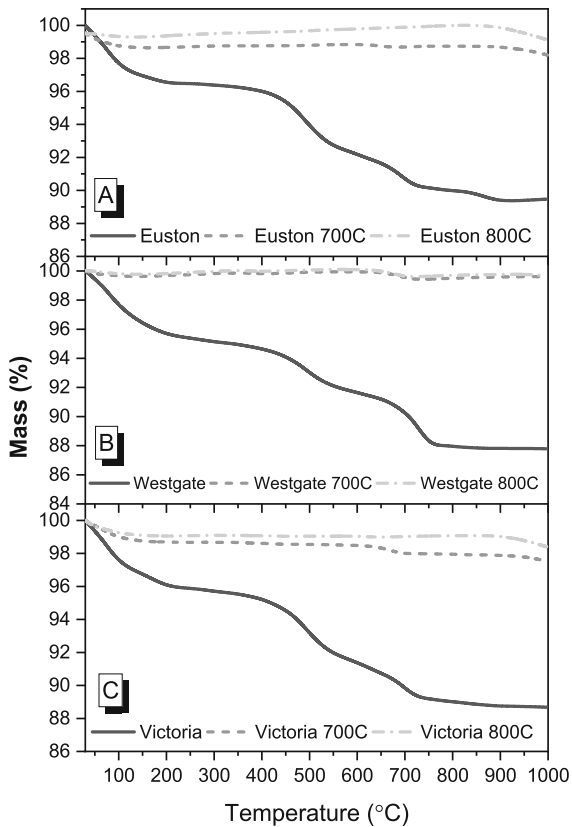
Fig. 7 Thermogravimetric curves, before and after calcination, for (**a**) Euston, (**b**) Westgate and (**c**) Victoria clays

Thames or Thames estuary, higher probability of chloride presence might be encountered.

The thermogravimetric, differential thermogravimetric curves (Fig. 7) and evolved gas curves (Fig. 8) support the findings from the XRD analysis (Fig. 6). Just as the presence of thermal mass loss event at a characteristic temperatures can indicate the presence of a given mineral [50], the absence of characteristic mass loss events can indicate the absence of a given mineral. Dehydroxylation of kaolinite was completed for all calcined clays, as seen from the absence of the peak with its centre at approximately 500 °C in the dTG (Fig. 8a, e, i) and H_2O (Fig. 8b, f, j) evolution curves. This is consistent with the XRD results discussed above. The majority of carbonate phases (mostly dolomite) decomposed after calcination at 700 °C [57], as seen from the reduction in magnitude of the peak centred at approximately 700 °C in the CO_2 evolution curves. Decomposition of carbonates seemed to be complete after calcination at 800°C in the Euston (Fig. 8c) and Victoria (Fig. 8k) clays, but a small amount of carbonates seemed to remain for Westgate 800°C (Fig. 8g). These observations are consistent with reduction in the intensity of the reflection associated with carbonate minerals identified by XRD (Fig. 6). Lastly, the conversion of pyrite to hematite in all the calcined clays was confirmed the
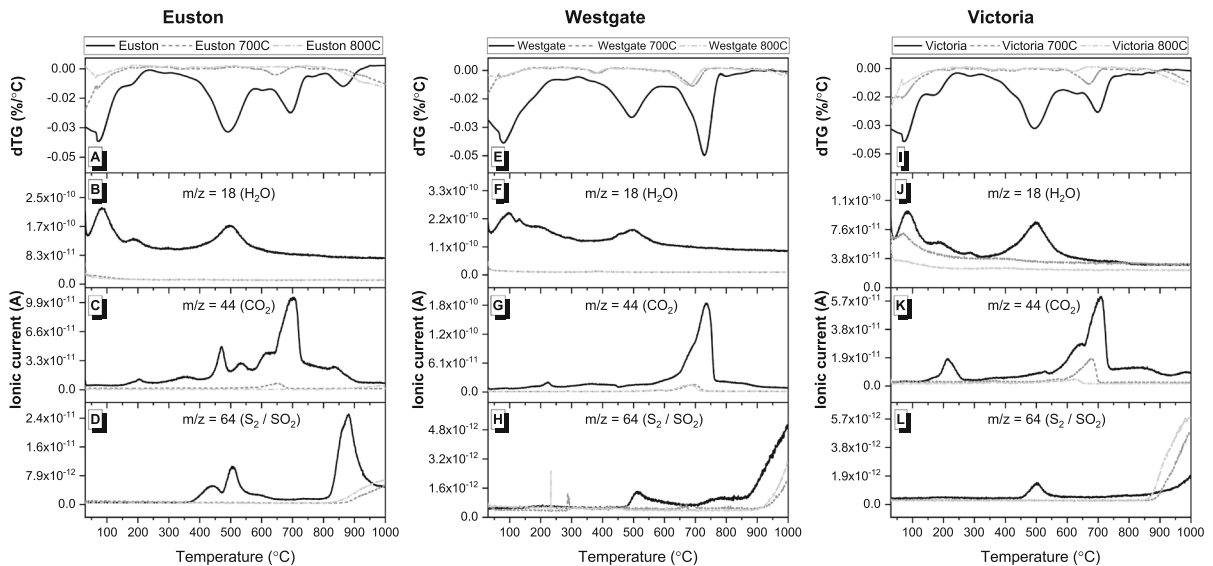
Fig. 8 dTG curves and H_2O, CO_2 and S_2/SO_2 mass spectrometry curves for (**a–d**) Euston, (**e–h**) Westgate, and (**i–l**) Victoria clays

Table 3 Mineralogical composition of the raw and calcined clays evaluated. Estimated phase quantities are stated in wt%, to a precision of 1 decimal place

	Westgate				Euston			Victoria		
	Raw	700 °C	800 °C	IC	Raw	700 °C	800 °C	Raw	700 °C	800 °C
Quartz	27.7	29.5	29.1	23.4	27.9	33.2	32.3	21.8	26	22.8
Kaolinite	15.5	0	0	0	15.1	0	0	17.9	0	0
Muscovite	45.3	40	38.4	35.3	43	33.4	35.9	45	49	43.8
Gypsum	0.9	0	0	0	0.7	0	0	0.6	0	0
Dolomite	1.6	0	0	0	1.8	0	0	1.7	0	0
Calcite	0.2	3.4	0.6	0.3	0.2	0	0	0.2	0	0
Microcline	5	9	8.6	9.8	4.6	11.3	10.4	4.5	8.3	9
Pyrite	0.6	0	0	0	0.6	0	0	0.7	0	0
Rutile	0.2	0.5	0.3	0	0.3	0.6	0.6	0.3	0.6	0.6
Hematite	0	0.9	1.2	1.0	0	1.1	1.5	0	1.3	1.5
Albite	2.4	1.5	1	0.4	2.2	2.3	1.9	1.2	2.2	2.1
Periclase	0	0	0.1	0	0	0	0	0	0	0
Lime	0	0	0.2	0.1	0	0	0	0	0.1	0.1
Amorphous content	0	15.3	20.2	29.6	3.3	18.1	17.4	5.6	12.3	20.1
Traces	0.6	–	0.3	0.1	0.3	0	0	0.5	0.2	–
Total	100	100	100	100	100	100	100	100	100	100
Goodness of Fit	2.9	3.0	2.8	2.2	2.9	3.3	3.00	2.6	3.2	2.7

absence of the peak centred around 500 °C in the S_2/SO_2 evolution curves—this is consistent with the XRD results (Fig. 6) and previous findings [38].

Table 3 summarises the mineralogical composition of the raw and calcined clays, as determined by semi-quantitative Rietveld XRD analysis. Estimated kaolinite content of the raw clays varied from 15 to 18 wt%. This is slightly lower than the range of 21–28 wt% kaolinite content estimated from TG results (Supplementary Information–Table S2). Part of this discrepancy may potentially be explained by an overlap between dehydroxylation of kaolinite, and dehydroxylation of other clay minerals present (which cannot be fully captured in the method used here to estimate uncertainty) [42]. Thus, whilst estimates from both XRD and TG give a broadly similar range, the TG results can be considered as a more optimistic upper limit. A further challenge around characterisation is difficulties in quantifying 2:1 clay minerals using conventional characterisation methods. Values for mineral contents estimated applying quantitative XRD data need to be interpreted carefully, due to inherent limitations of this techniques and unavoidable

uncertainties in the analysis process [58]. For example, the lack of suitable structural files hinders the quantification of smectite and illite clay minerals. Therefore, the estimated values for mineral contents in Table 3 should be considered as semi-quantitative.

Overall, the mineralogical changes in the clays after calcination were broadly similar, with some small differences. Complete dehydroxylation of kaolinite was achieved for both calcination temperatures, across all London Clays. Pyrite and dolomite were not detected in the calcined clays, due to thermal decomposition of these phases during calcination. Whilst the majority of carbonates were decomposed after calcination at both temperatures, small amounts did remain in some cases. Pyrite is a mineral known for its detrimental expansive behaviour in concrete [59, 60]. If calcination temperatures are not high enough to cause its decomposition to hematite, then it could be a cause of concern. In this study, decomposition of pyrite was achieved for both 700 and 800 °C, across all source clays. Industrial calcined (IC) Westgate soil has a marginally higher amorphous content from the

larger batch of materials that was calcined industrially in a rotary kiln.

3.4 Chemical reactivity of calcined clays

The R^3 testing results of the calcined clays evaluated are reported in Fig. 9. In each case, clays calcined at 800 °C exhibited slightly higher heat flow values between 1 and 4 days after mixing (Fig. 9a). This resulted in a modest increase in 7-day cumulative heat for clays calcined at 800 °C, compared to 700 °C (Fig. 9b). For equivalent calcination temperatures, the Euston clays had slightly higher reactivity values than the Westgate clays. This could be due to the Euston clay having a combination of a slightly higher kaolinite content (Supplementary Information– Table S2) and slightly finer particle size distribution (Supplementary Information–Table S3) compared to the Westgate clay.

The 7-day cumulative heat values for all the calcined clays are listed in Table S4 in the Supplementary Information file. Robustness testing of the R^3 test methods established the single operator coefficient of variance for 7-day cumulative heat to be 2.3% [61]. For the range of 7-day cumulative heat values, this corresponds to a standard deviation in the range of 5.4–7.1 J/(g of SCM). The magnitude of the difference between the clays calcined at 800 and 700 °C is 67.2 and 75.9 J/(g of SCM), for the Euston and Westgate clays respectively. Because these differences did not

fall within the expected range of single operator variation, they were considered to represent meaningful differences in the measured reactivity. From the 7-day cumulative heat values (Supplementary Information–Table S4), all the calcined clays meet the 90% confidence threshold to classify as "moderately reactive calcined clays" (i.e. > 190 J/(g of SCM)) considering the thresholds recommended by Londono-Zuluaga et al.[46]. Out of the three clays investigated, the Westgate clay was selected to industrially produce a pilot-scale batch on the basis of logistical convenience of sourcing larger quantities of material within the planned works schedule. Given the similar mineralogy and reactivity performance of the three clays, one clay was deemed to be sufficiently representative to take forward for development of blend formulations.

The estimates of amorphous content from quantitative XRD (Table 3) are consistent with the observations from R^3 reactivity data. R^3 reactivity measurements on an industrially sourced, high purity metakaolin found the 7-day cumulative heat value to be 1150 J/g of SCM (Fig. 9b). The six calcined London Clays considered in this study yielded 7-day cumulative heat values in the range of 234.5–329.0 J/g of SCM (Supplementary Information–Table S4). These values lie in the range of 20–30% of the value for the high-purity metakaolin (as highlighted in the Fig. 9). The amorphous content estimates of approximately 12–20% made via Rietveld refinement are
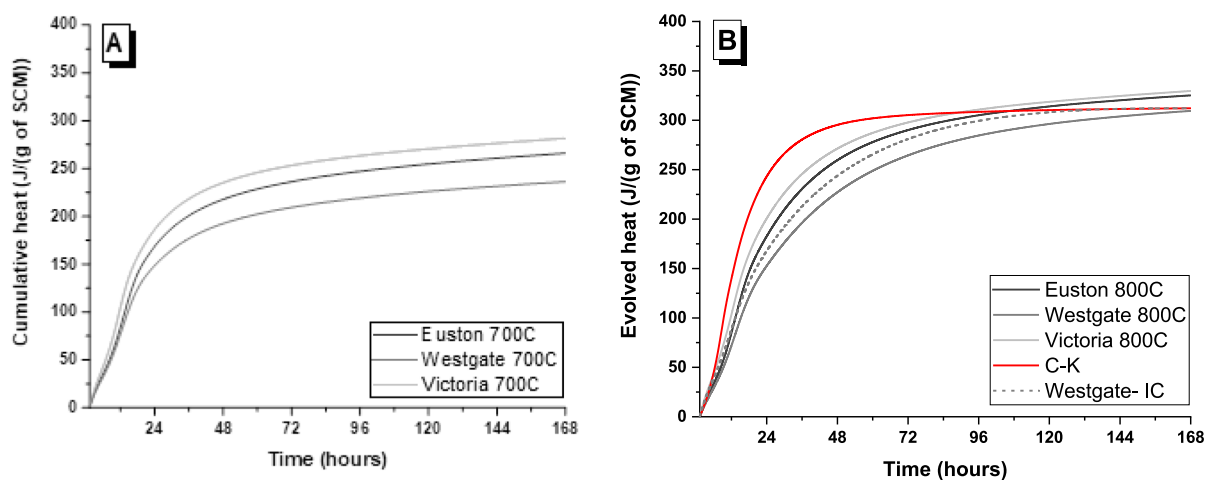
Fig. 9 Isothermal calorimetry cumulative heat curves of all the clays as a function of the calcination temperature, where (**A**) corresponds to clays calcined at 700 °C and (**B**) corresponds to clays calcined at 800 °C. C-K, a kaolinitic clay with similar kaolinite content to the London clays, was calcined at 800 °C— it is plotted here as a reference curve

thus broadly consistent with the observations from cumulative heat data.

The overall R^3 results for C–K are consistent with the calcined London clays reactive content identified in this material. The reference kaolinitic clay (C–K calcined at 800 °C) was chosen as the clay contained only quartz along with 27 wt% kaolinite content. However, it is interesting to observe differences in the gradients of the cumulative heat curves over different time periods between kaolinite only clay and mixed London Clay. This highlights the difference in the contribution to chemical reactivity from reactive phases formed from different minerals i.e., only kaolinite (as in C–K) and kaolinite along with other clays minerals (as in three London clays considered in this study). The reaction kinetics during the R^3 test are slower for the calcined London Clays compared to the K–C reference kaolinite clay within the first 48 h (Fig. 9b). However, beyond the first 48 h, the calcined London Clays seem to react more quickly than the K-C reference kaolinite clay. This is likely associated with the content of 2:1 minerals in the London Clays—calcined 2:1 clay minerals are expected to exhibit slower dissolution characteristics compared to metakaolin [62, 63].

In order to elucidate the contribution of calcined 2:1 minerals to chemical reactivity of the calcined clays studied, a reference system was used. Testing reactivity of metakaolins of controlled purity, by blending an industrially sourced high purity metakaolin with quartz, gives a hypothetical trend line for reactivity expected from metakaolinite content alone (Fig. 10). This makes possible to infer whether the presence of the calcined 2:1 clay minerals makes a contribution to reactivity above and beyond that expected from kaolinite alone.

The horizontal arrows in Fig. 10 extrapolate the hypothetical kaolinite content from the experimentally observed 7-day cumulative heat for the calcined London Clays. While the kaolinite content of the raw clays (determined via quantitative XRD, Table 3) were in the range of only 15–20%, calcined London Clays have a reactivity potential equivalent to kaolinite content of maximum 30% (using the trendline generated from the reference metakaolins) due to the contribution from other clay minerals. Whilst the R^3 reactivity test offer insights into the overall chemical reactivity associated with the kaolinite content in the raw clay, a degree of caution is needed in interpreting this analysis. As described in Sect. 3.4, the cumulative heat curves in Fig. 9 show that the calcined London Clays continue to react beyond 7 days, in a way that the C–K reference clay did not. Given the slower reaction kinetics of mixed clays, due to their 2:1 mineral content, the R^3 test may slightly underestimate the reactivity of mixed clays in practice, if run only for 7 days as recommended by the standard.

The notion of what constitutes an 'optimal' calcination temperature when processing a given source clay is open to debate. R^3 tests make it straightforward

Fig. 10 7 day cumulative heat determined via R^3 test as a function of kaolinite content. Values from the calcined London Clays are plotted on the y-axis, assuming 'zero' kaolinite content for analysis purposes. The linear best fit line is based on the R^3 test results of tailor-made calcined clays containing 20, 40, 60, 80, 100% of a high-purity metakaolin, diluted with quartz
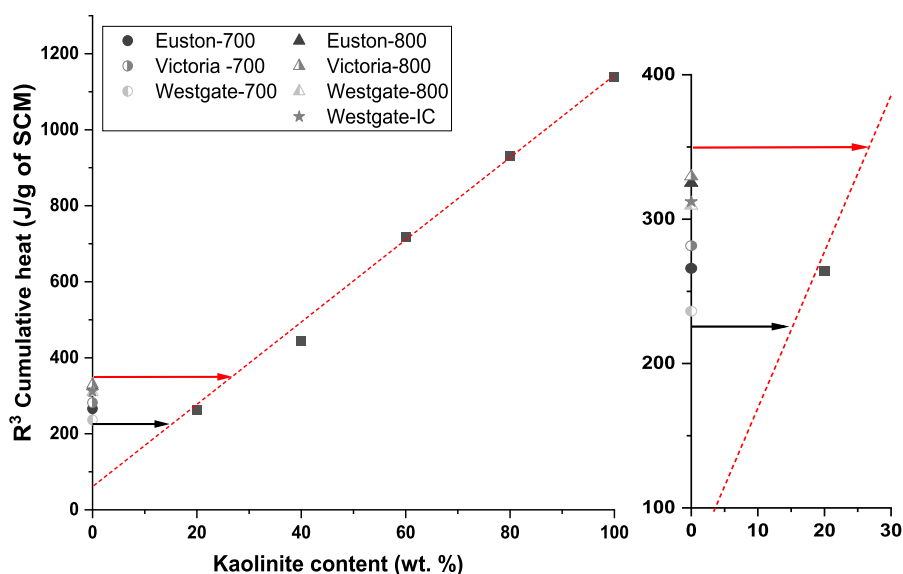
to make a quantitative comparison of chemical reactivity at different temperatures. And yet, chemical reactivity is only one of the factors that needs to be considered when deciding on a calcination temperature in these systems. Two other factors are the formation of expansive phases resulting from the thermal decomposition of carbonate minerals (i.e. calcite and dolomite), and the impact of the resultant process emissions on the overall embodied carbon of the calcined clay.

Previous studies have identified a trade-off between an increased dehydroxylation of 2:1 clay minerals (beneficial to reactivity), and decomposition of carbonate phases (deleterious to reactivity) [18, 51]. In this study, the majority of carbonates were decomposed after calcination for all clays at both 700 and 800 °C, although small amounts did remain in some cases. The decomposition pathway of dolomite is distinct from calcite, and merits special attention. Dolomite thermal decomposition leads to an increase in calcite content along with potential formation of MgO and release of CO_2; if calcite is present in a calcined clay after calcination, this could produce an aluminate-carbonate reaction leading to formation of carboaluminates in hydrated cement matrix. However, negligible amounts of free lime and periclase were identified in the XRD patterns after calcination at both 700 and 800 °C.

For the type of carbonate minerals in the three sources of London Clay studied herein, the additional carbon footprint (relative to a clay without any carbonate minerals) associated with the decomposition of carbonate minerals was estimated to be in the range of 24–42 kg/tonne of calcined clay. In comparison, a typical embodied carbon of thermal treatment is estimated to be at least 240 kg/tonne [41]. Therefore, decomposition of carbonate minerals is likely to make a minor, rather non-negligible, contribution to the overall embodied carbon of the processing of London Clay specifically and calcined clays in general.

In the case of the sources of London Clay evaluated in this study, the minor quantity of carbonate minerals (estimated < 10 wt%) suggest that there is more to gain than to lose by calcining at a higher temperature of 800 °C. More reactive material might lead to higher CEM I replacement levels for comparable strength developments, offsetting the embodied carbon associated with the decarbonation of carbonate minerals during calcination. However, this should not be

extrapolated as a universal finding across mixed clays. For clays with a high content of carbonates and a lower content of clay minerals, it may be the case that a slightly lower calcination temperature is more favourable on balance.

### 3.5 Blend cement formulations optimisation

A high volume replacement of CEM I with SCMs is known to create a sulphate demand due to additional aluminates and surface area introduced by the SCM that affect early age hydration kinetics of clinker phases [64–66]. Hence it is important to check for sulphate demand to ensure blends prepared with calcined London Clay is formulated to ensure maximum reaction potential at early age. The heat flow curves for the CC50 (Fig. 11a) and CC70 (Fig. 12a) series both exhibited a similar trend—the aluminate peak shifted to later times with increasing gypsum content. At 24 h, the pastes with 1 wt% gypsum exhibited the highest heat flow values for both CC50 and CC70 series. The heat release values were lower for the CC70 series due to higher replacement level of CEM I. Values of cumulative heat at 24 h were also marginally highest for the 1wt% gypsum addition (Fig. 13). It would therefore be expected that the 1 wt% gypsum addition blends would exhibit higher 1-day strength. The gypsum demand did not change with the increase in replacement level from 50 to 70 wt%. This is mainly due to the relatively low metakaolin content of the industrially calcined Westgate clay.

The optimised gypsum addition for both CC50 and CC70 was therefore identified to be 1 wt%. Setting time measurements were carried out for both these optimised blends (i.e. CC50-G1 and CC70-G1), and compared to CEM I (Fig. 14). The setting window for CC50-G1 and CC70-G1 is 6–8 h. CC70-G1 is marginally faster setting than CC50-G1, and both blends exhibit noticeably accelerated setting relative to CEM I despite a delay in heat release observed from calorimetry. In this case, normliased heat flow per gram of Portland cement was able to confirm the acceleration in reaction kinetics; although heat flow per gram of paste does not showcase any acceleration of reaction. Similar reduction in setting time has been observed with other calcined clays in previous studies, attributed to the addition of calcined clay increasing the cohesivity of the mixes and heterogenous
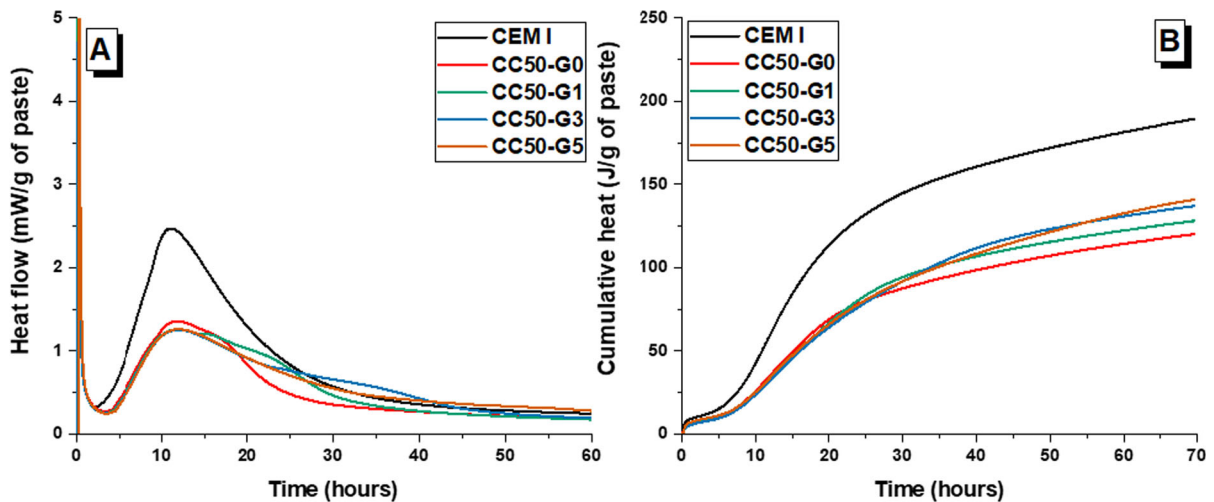
Fig. 11 Isothermal calorimetry results of blended calcined London Clay binders showing the influence of gypsum addition (0–5 wt%) on (**A**) heat flow, and (**B**) cumulative heat, for the CC-50 series
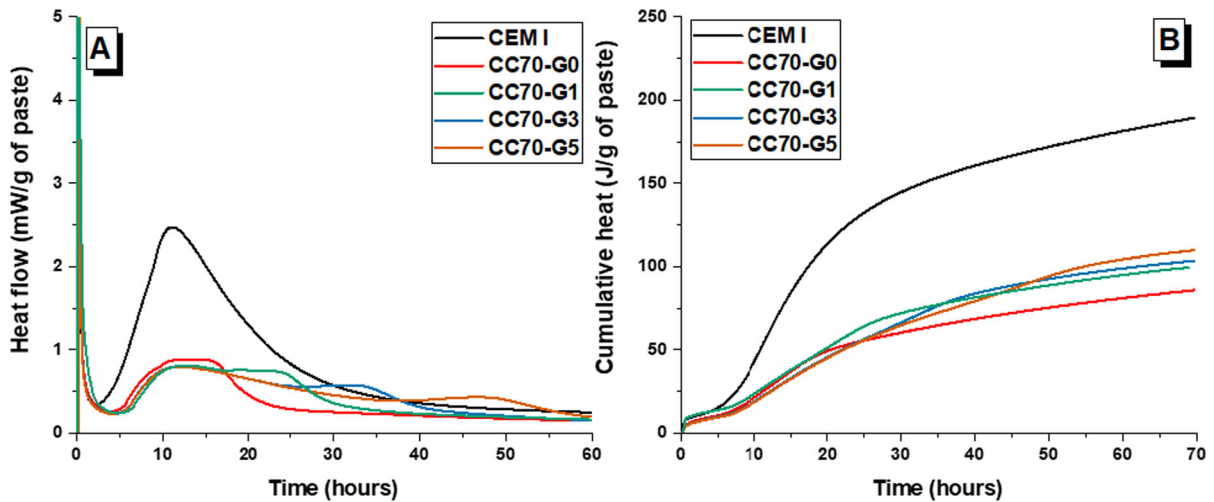

Fig. 12 Isothermal calorimetry results of blended calcined London Clay binders showing the influence of gypsum addition (0–5 wt%) on (**A**) heat flow, and (**B**) cumulative heat, for the CC-70 series

nucleation of calcium aluminosilicate hydrate (C–A–S–H) on fine calcined clay particles at early ages [67].

3.6 Compressive strength development

The compressive strength values (Fig. 15). were consistently lower for the CC70 series, compared to the CC50 series. As expected, increased w/b ratio resulted in a decrease in compressive strength, across both replacement levels. The addition of calcined clay often contributes to strength increase within 7 days of curing [29, 68, 69], and the results reported here are consistent with what has been observed in other calcined clays blended systems [67]. However, it is worth mentioning that all these studies have reported minimal strength development after 28 days while with calcined London Clay there is considerable strength development after 28 days, probably due to the slower reactivity.
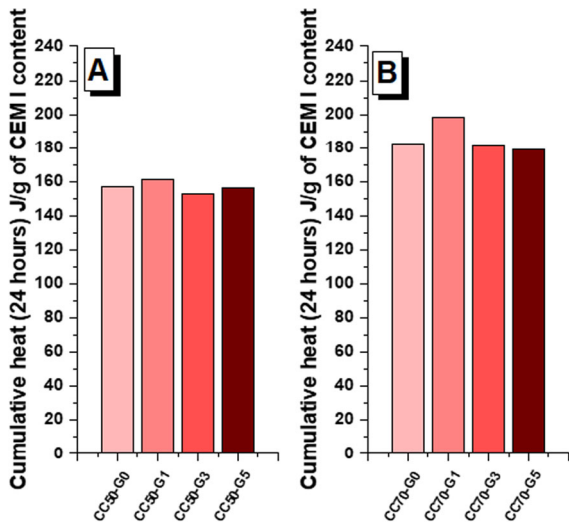
Fig. 13 Cumulative heat normalised by CEM I content at 24 h for (**A**) CC-50 series, and (**B**) CC-70 series, as a function of gypsum addition in the mix (0–5 wt%)
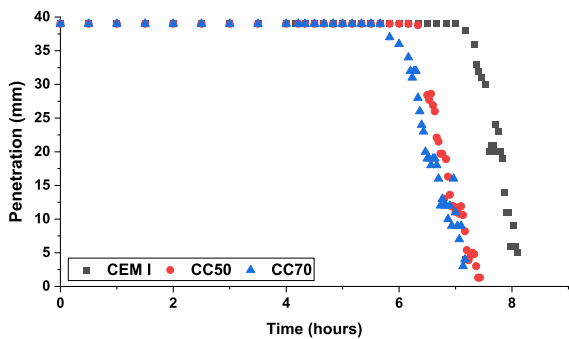
Fig. 14 Setting time curves for CEM I, CC50 and CC70 blends (both with 1% gypsum addition). All pastes were designed with w/b = 0.5
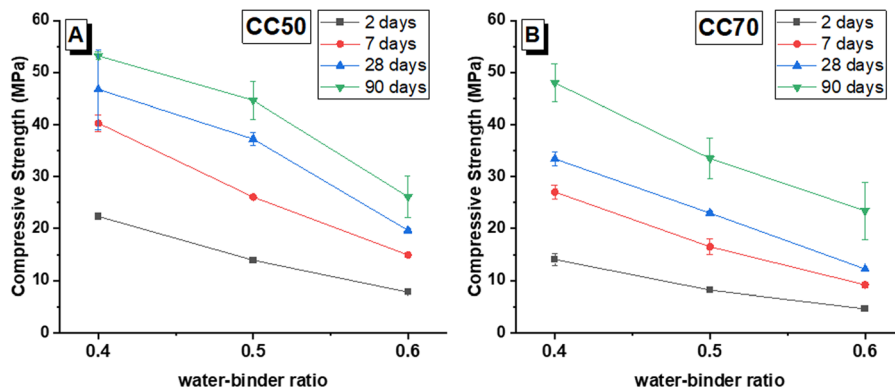
4 Conclusions and recommendations

The rich variety inherent in naturally occurring clay resources offers numereous potential for SCM production; but it also presents challenges. On the one hand, this study shows that 800 °C is an effective calcination temperature for London Clays, in terms of reactivity performance and avoiding potentially problematic mineral phases. However, it is also highlighted that care is needed in characterisation work and decision-making. Whilst XRD and TG are techniques familiar to those in the cement industry, quantifying the presence of 2:1 clay minerals and a range of associated minerals is not straightforward. R^3 reactivity cumulative heat results showcase the chemical reactivity of calcined excavated London Clay. Its potential as a material suitable for SCM usage was validated by the compressive strength development of blended cements produced with them.

London Clay samples from three different locations displayed very similarly behaviour, despite being sourced several kilometres away from each other. Whilst geological surveys can offer valuable insights into the expected mineralogy of excavated material in a given area, detailed characterisation is still necessary for quality control. Whilst many of the principles around characterisation and selection of calcination temperature are more-or-less universal, these formation-specific findings of the present stuidy on London Clay cannot be transferred wholesale to other geological resources (e.g., Oxford Clays, Etruvia Marls) without further validation. The R^3 results showed that the 2:1 clay minerals present in London Clays react

Fig. 15 Compressive strength evolution as a function of curing time and w/b ratio of the optimised blends (**A**) CC50, and (**B**) CC70. Error bars correspond to one standard deviation

more slowly than conventional kaolinitic clays, and that they may be making a non-negligible contribution to reactivity at 7 days and possibly beyond. Therefore, it is recommended to extend the R^3 testing duration to 14 days for these type clays, to avoid underestimating the true potential chemical reactivity of these materials.

Compressive strength results from optimised blended formulations indicate that high levels of CEM I substitution (up to 70 wt%) by calcined London Clays are achievable for the potential production of concretes of different strength grades. Work is currently underway to develop further understanding on designing blended cements, and conducting concrete mixes trials using calcined London Clay SCM. Whilst low-risk applications will be the starting point for concretes made with calcined London Clay, durability monitoring in natural exposure conditions will still be essential for validating performance of these concretes in service.

The notion of 'technological robustness' will be critical to the use of excavated materials for calcined clay production. The flexibility and versatility of on-site production is highly attractive as an agile approach to waste minimisation and valorisation. However, this alternative production model, in contrast to centralised, static production at a large clay deposit, has the flipside of more attention needed to characterising the excavated materials and their variability to control the quality of the materials produced from different construction sites.

Author contributions YD–Investigation, Formal Analysis, Investigation, Writing–Original Draft, Funding acquisition; ATMM–Investigation, Formal Analysis, Investigation, Writing–Original Draft, Funding acquisition; SR–Investigation, Formal Analysis; FK–Conceptualisation, Resources; Writing—Review & Editing, Project administration, Funding acquisition; AP—Resources; Writing—Review & Editing, Project administration, Funding acquisition; SAB–Conceptualization, Methodology, Formal Analysis, Writing–Review & Editing, Supervision, Project Administration, Funding acquisition.

References

1. Zhang C, Hu M, Di Maio F et al (2022) An overview of the waste hierarchy framework for analyzing the circularity in construction and demolition waste management in Europe. Sci Total Environ 803:149892. https://doi.org/10.1016/j.scitotenv.2021.149892

2. The Green Construction Board (2021) The Routemap for Zero Avoidable Waste in Construction (https://www.constructionleadershipcouncil.co.uk/wp-content/uploads/2021/07/ZAW-Interactive-Routemap-FINAL.pdf)

3. Katsumi T (2015) Soil excavation and reclamation in civil engineering: environmental aspects. Soil Sci Plant Nutr 61:22–29. https://doi.org/10.1080/00380768.2015.1020506

4. Haas M, Mongeard L, Ulrici L, d'Aloïa L, Cherrey A, Galler R, Benedikt M (2021) Applicability of excavated rock material: a European technical review implying opportunities for future tunnelling projects. J Clean Prod 315:128049. https://doi.org/10.1016/j.jclepro.2021.128049

5. Magnusson S, Lundberg K, Svedberg B, Knutsson S (2015) Sustainable management of excavated soil and rock in urban areas – a literature review. J Clean Prod 93:18–25. https://doi.org/10.1016/j.jclepro.2015.01.010

6. Low Carbon Concrete Group,   The Green Construction Board (2022) Low carbon concrete routemap: setting the agenda for a path to net zero. Institute of Civil Engineers, London   (https://www.ice.org.uk/media/q12jkljj/low-carbon-concrete-routemap.pdf)

7. Shah IH, Miller SA, Jiang D, Myers RJ (2022) Cement substitution with secondary materials can reduce annual

global CO_2 emissions by up to 1.3 gigatons. Nat Commun 13:5758. https://doi.org/10.1038/s41467-022-33289-7

8. Alberici S, Beer J de, Hoorn I van der, Staats M (2017) Fly ash and blast furnace slag for cement manufacturing,Department for Business, Energy and Industrial Strategy (BEIS), London, U.K. Department for Business, Energy and Industrial Strategy, London, U.K

9. Sánchez Berriel S, Favier A, Rosa Domínguez E et al (2016) Assessing the environmental and economic potential of Limestone Calcined Clay Cement in Cuba. J Clean Prod 124:361–369. https://doi.org/10.1016/j.jclepro.2016.02.125

10. Gettu R, Patel A, Rathi V et al (2019) Influence of supplementary cementitious materials on the sustainability parameters of cements and concretes in the Indian context. Mater Struct 52:1–11. https://doi.org/10.1617/s11527-019-1321-5

11. Bediako M, Valentini L (2022) Strength performance and life cycle assessment of high-volume low-grade kaolin clay pozzolan concrete: a Ghanaian scenario. Case Stud Constr Mater 17:e01679. https://doi.org/10.1016/j.cscm.2022.e01679

12. Salvador S, Pons O (2000) A semi-mobile flash dryer/calciner unit to manufacture pozzolana from raw clay soils — application to soil stabilisation. Constr Build Mater 14:109–117. https://doi.org/10.1016/S0950-0618(00)00005-2

13. Hago AW, Al-Rawas AA (2008) Design of a rotary kiln for production of Sarooj. J Eng Res [TJER] 5:55–61. https://doi.org/10.24200/tjer.vol5iss1pp55-61

14. Kanavaris F, Papakosta A, Zunino F, Pantelidou H, Baudet B, Marsh ATM, Rahmon S, Dhandapani Y, Bernal SA, Szanser J, Tsoumelekas A (2022) Suitability of excavated London Clay from tunnelling operations as a supplementary cementitious material and expanded clay aggregate. In: Proceedings of the International Conference on Calcined Clays for Sustainable Concrete (CCSC 2022). Sharma M, Hafez H, Zunino F, Scrivener KL (Eds). pp 3–4

15. Hossain MU, Thomas Ng S (2019) Influence of waste materials on buildings' life cycle environmental impacts: adopting resource recovery principle. Resour Conserv Recycl 142:10–23. https://doi.org/10.1016/j.resconrec.2018.11.010

16. Kanavaris F, Papakosta A (2022) Calcining excavated London Clay to produce supplementary cementitious material and lightweight aggregate. Concrete Magazine, Jul, pp 40–42

17. Zhou D (2016) Developing supplementary cementitious materials from waste london clay. PhD thesis, Imperial College London, UK

18. Zhou D, Wang R, Tyrer M, Wong H, Cheeseman C (2017) Sustainable infrastructure development through use of calcined excavated waste clay as a supplementary cementitious material. J Clean Prod 168:1180–1192. https://doi.org/10.1016/j.jclepro.2017.09.098

19. Priyadharshini P, Ramamurthy K, Robinson RG (2018) Reuse potential of stabilized excavation soil as fine aggregate in cement mortar. Constr Build Mater 192:141–152. https://doi.org/10.1016/j.conbuildmat.2018.10.141

20. Morel JC, Charef R, Hamard E, Fabbri A, Beckett C, Bui QB (2021) Earth as construction material in the circular economy context: practitioner perspectives on barriers to overcome. Philos Trans R Soc 376:20200182. https://doi.org/10.1098/rstb.2020.0182

21. Ardant D, Brumaud C, Perrot A, Habert G (2023) Robust clay binder for earth-based concrete. Cem Concr Res 172:107207. https://doi.org/10.1016/j.cemconres.2023.107207

22. Cristelo N, Coelho J, Oliveira M et al (2020) Recycling and application of mine tailings in alkali-activated cements and mortars—strength development and environmental assessment. Appl Sci 10:2084. https://doi.org/10.3390/app10062084

23. Julphunthong P, Joyklad P (2019) Utilization of several industrial wastes as raw material for calcium sulfoaluminate cement. Mater 12:3319. https://doi.org/10.3390/ma12203319

24. Kleib J, Amar M, Benzerzour M, Abriak N-E (2022) Effect of flash-calcined sediment substitution in sulfoaluminate cement mortar. Front Mater 9:1035551. https://doi.org/10.3389/fmats.2022.1035551

25. Mellings L, Limna G (2017) Crossrail learning legacy - Excavated materials story. https://learninglegacy.crossrail.co.uk/documents/excavated-materials-story/

26. Munro A (2021) HS2 railway, UK – why the country needs it. 174:3–11. https://doi.org/10.1680/jtran.18.00040

27. Kemp SJ, Wagner D (2006) The mineralogy, geochemistry and surface area of mudrocks from the London Clay Formation of southern England. British Geological Survey, Keyworth, Nottingham

28. Scrivener K, Martirena F, Bishnoi S, Maity S (2018) Calcined clay limestone cements (LC3). Cem Concr Res 114:49–56. https://doi.org/10.1016/j.cemconres.2017.08.017

29. Avet F, Scrivener K (2018) Investigation of the calcined kaolinite content on the hydration of Limestone Calcined Clay Cement (LC3). Cem Concr Res 107:124–135. https://doi.org/10.1016/j.cemconres.2018.02.016

30. Fernandez R, Martirena F, Scrivener KL (2011) The origin of the pozzolanic activity of calcined clay minerals: a comparison between kaolinite, illite and montmorillonite. Cem Concr Res 41:113–122. https://doi.org/10.1016/j.cemconres.2010.09.013

31. He C, Makovicky E, Osbæck B (1996) Thermal treatment and pozzolanic activity of Na- and Ca-montmorillonite. Appl Clay Sci 10:351–368. https://doi.org/10.1016/0169-1317(95)00037-2

32. He C, Osbaeck B, Makovicky E (1995) Pozzolanic reactions of six principal clay minerals: activation, reactivity assessments and technological effects. Cem Concr Res 25:1691–1702. https://doi.org/10.1016/0008-8846(95)00165-4

33. Hollanders S, Adriaens R, Skibsted J, Cizer Ö, Elsen J (2016) Pozzolanic reactivity of pure calcined clays. Appl Clay Sci 132–133:552–560. https://doi.org/10.1016/j.clay.2016.08.003

34. Maier M, Beuntner N, Thienel K-C (2021) Mineralogical characterization and reactivity test of common clays suitable as supplementary cementitious material. Appl Clay Sci 202:105990. https://doi.org/10.1016/j.clay.2021.105990

35. Ayati B, Newport D, Wong H, Cheeseman C (2022) Low-carbon cements: Potential for low-grade calcined clays to

form supplementary cementitious materials. Clean Mater 5:100099. https://doi.org/10.1016/j.clema.2022.100099

36. Deng M, Hong D, Lan X, Tang M (1995) Mechanism of expansion in hardened cement pastes with hard-burnt free lime. Cem Concr Res 25:440–448. https://doi.org/10.1016/0008-8846(95)00030-5

37. Courard L, Degée H, Darimont A (2014) Effects of the presence of free lime nodules into concrete: experimentation and modelling. Cem Concr Res 64:73–88. https://doi.org/10.1016/j.cemconres.2014.06.005

38. Zunino F, Scrivener K (2021) Oxidation of pyrite (FeS$_2$) and troilite (FeS) impurities in kaolinitic clays after calcination. Mater Struct 55:9. https://doi.org/10.1617/s11527-021-01858-9

39. BSI BS 1377-1:2016 (2016) Methods of test for soils for civil engineering purposes. General requirements and sample preparation

40. BSI BS 1377-2:1990 (1990) Methods of test for soils for civil engineering purposes. Classification tests

41. Hanein T, Thienel K-C, Zunino F et al (2021) Clay calcination technology: state-of-the-art review by the RILEM TC 282-CCL. Mater Struct 55:3. https://doi.org/10.1617/s11527-021-01807-6

42. Snellings R, Reyes RA, Hanein T, Irassar EF, Kanavaris F, Maier M, Marsh ATM, Valentini L, Zunino F, Alujas Diaz A (2022) Paper of RILEM TC 282-CCL: mineralogical characterization methods for clay resources intended for use as supplementary cementitious material. Mater Struct 55:149. https://doi.org/10.1617/s11527-022-01973-1

43. Warr LN (2020) Recommended abbreviations for the names of clay minerals and associated phases. Clay Miner 55:261–264. https://doi.org/10.1180/clm.2020.30

44. Palacios M, Kazemi-Kamyab H, Mantellato S, Bowen P (2018) Laser diffraction and gas adsorption techniques. In: Scrivener K, Snellings R, Lothenbach B (eds) A practical guide to microstructural analysis of cementitious materials. CRC Press, Boca Raton, FL, pp 445–483

45. ASTM C1897 − 20 (2020). Standard test methods for measuring the reactivity of supplementary cementitious materials by isothermal calorimetry and bound water measurements

46. Londono-Zuluaga D, Gholizadeh-Vayghan A, Winnefeld F et al (2022) Report of RILEM TC 267-TRM phase 3: validation of the R^3 reactivity test across a wide range of materials. Mater Struct 55:142. https://doi.org/10.1617/s11527-022-01947-3

47. BSI BS EN 12390-3:2019 (2019) Testing hardened concrete. Compressive strength of test specimens

48. Dhandapani Y, Rahmon S, Marsh ATM, et al (2022) Fresh state properties of low clinker cement made of excavated London Clay from tunnelling operations. In proceedings of the 41st IoM^3 Cement and Concrete Science Conference. Leeds, UK

49. Alujas Diaz A, Almenares Reyes RS, Hanein T et al (2022) Properties and occurrence of clay resources for use as supplementary cementitious materials. Mater Struct 55:139. https://doi.org/10.1617/s11527-022-01972-2

50. Földvári M (2011) Handbook of thermogravimetric system of minerals and its use in geological practice. Geological Institute of Hungary, Budapest

51. Zunino F, Boehm-Courjault E, Scrivener K (2020) The impact of calcite impurities in clays containing kaolinite on their reactivity in cement after calcination. Mater Struct 53:44. https://doi.org/10.1617/s11527-020-01478-9

52. Avet F, Scrivener K (2020) Simple and reliable quantification of kaolinite in clay using an oven and a balance. In: Calcined clays for sustainable concrete: proceedings of the 3rd international conference on calcined clays for sustainable concrete. Springer Singapore, Singapore, pp 147–156

53. BRE Construction Division (2005) Concrete in aggressive ground - Special Digest 1:2005

54. Hobbs DW (2003) Thaumasite sulfate attack in field and laboratory concretes: implications for specifications. Cem Concr Compos 25:1195–1202. https://doi.org/10.1016/S0958-9465(03)00145-8

55. Hobbs DW, Taylor MG (2000) Nature of the thaumasite sulfate attack mechanism in field concrete. Cem Concr Res 30:529–533. https://doi.org/10.1016/S0008-8846(99)00255-0

56. Duchesne J, Rodrigues A, Fournier B (2021) Concrete damage due to oxidation of pyrrhotite-bearing aggregate: a review. RILEM Tech Lett 6:82–92. https://doi.org/10.21809/rilemtechlett.2021.138

57. McIntosh RM, Sharp JH, Wilburn FW (1990) The thermal decomposition of dolomite. Thermochim Acta 165:281–296. https://doi.org/10.1016/0040-6031(90)80228-Q

58. Snellings R (2018) X-ray powder diffraction applied to cement. In: Scrivener K, Snellings R, Lothenbach B (eds) A practical guide to microstructural analysis of cementitious materials. CRC Press, Boca Raton, FL, pp 104–176

59. Schmidt T, Leemann A, Gallucci E, Scrivener K (2011) Physical and microstructural aspects of iron sulfide degradation in concrete. Cem Concr Res 41:263–269. https://doi.org/10.1016/j.cemconres.2010.11.011

60. Caparro APB, Braga V, de Medeiros MHF, Hoppe Filho J, Bragança MO, Portella KF, de Oliveira IC (2017) Internal attack by sulphates in cement pastes and mortars dosed with different levels of pyrite. J Build Pathol Rehabil 2:7. https://doi.org/10.1007/s41024-017-0026-9

61. Avet F, Li X, Ben Haha M, Bernal SA, Bishnoi S, Cizer Ö, Cyr M, Dolenec S, Durdzinski P, Haufe J, Hooton D, Juenger MCG, Kamali-Bernard S, Londono-Zuluaga D, Marsh ATM, Marroccoli M, Mrak M, Parashar A, Patapy C, Pedersen M, Provis JL, Sabio S, Schulze S, Snellings R, Telesca A, Thomas M, Vargas F, Vollpracht A, Walkley B, Winnefeld F, Ye G, Zhang S, Scrivener K (2022) Report of RILEM TC 267-TRM: optimization and testing of the robustness of the R3 reactivity tests for supplementary cementitious materials. Mater Struct 55:92. https://doi.org/10.1617/s11527-022-01928-6

62. Werling N, Kaltenbach J, Weidler PG et al (2022) Solubility of calcined kaolinite, montmorillonite, and illite in high molar NaOH and suitability as precursors for geopolymers. Clays Clay Miner 70:270–289. https://doi.org/10.1007/s42860-022-00185-6

63. Bauer A, Berger G (1998) Kaolinite and smectite dissolution rate in high molar KOH solutions at 35° and 80°C. Appl Geochem 13:905–916. https://doi.org/10.1016/S0883-2927(98)00018-3

64. Andrade Neto JS, De la Torre AG, Kirchheim AP (2021) Effects of sulfates on the hydration of Portland cement – a review. Constr Build Mater 279:122428. https://doi.org/10.1016/j.conbuildmat.2021.122428

65. Zunino F, Scrivener K (2022) Insights on the role of alumina content and the filler effect on the sulfate requirement of PC and blended cements. Cem Concr Res 160:106929. https://doi.org/10.1016/j.cemconres.2022.106929

66. Maier M, Sposito R, Beuntner N, Thienel K-C (2022) Particle characteristics of calcined clays and limestone and their impact on early hydration and sulfate demand of blended cement. Cem Concr Res 154:106736. https://doi.org/10.1016/j.cemconres.2022.106736

67. Dhandapani Y, Santhanam M, Gettu R, et al (2020) Perspectives on blended cementitious systems with calcined clay- limestone combination for sustainable low carbon cement transition. Indian Concr J 25–38. https://www.icjonline.com/explore_journals/2020/02/

68. Antoni M, Rossen J, Martirena F, Scrivener K (2012) Cement substitution by a combination of metakaolin and limestone. Cem Concr Res 42:1579–1589. https://doi.org/10.1016/j.cemconres.2012.09.006

69. Dhandapani Y, Sakthivel T, Santhanam M et al (2018) Mechanical properties and durability performance of concretes with Limestone Calcined Clay Cement (LC3). Cem Concr Res 107:136–151. https://doi.org/10.1016/j.cemconres.2018.02.005